Cell Mol Neurobiol (2017) 37:145–154
DOI 10.1007/s10571-016-0354-3

ORIGINAL RESEARCH

Primary Cilia in the Murine Cerebellum and in Mutant Models of Medulloblastoma

Chiara Di Pietro[1] · Daniela Marazziti[1] · Gina La Sala[1] · Zeinab Abbaszadeh[1] · Elisabetta Golini[1] · Rafaele Matteoni[1] · Glauco P. Tocchini-Valentini[1]

Received: 11 November 2015 / Accepted: 22 February 2016 / Published online: 2 March 2016

Abstract Cellular primary cilia crucially sense and transduce extracellular physicochemical stimuli. Cilium-mediated developmental signaling is tissue and cell type specific. Primary cilia are required for cerebellar differentiation and sonic hedgehog (Shh)-dependent proliferation of neuronal granule precursors. The mammalian G-protein-coupled receptor 37-like 1 is specifically expressed in cerebellar Bergmann glia astrocytes and participates in regulating postnatal cerebellar granule neuron proliferation/differentiation and Bergmann glia and Purkinje neuron maturation. The mouse receptor protein interacts with the patched 1 component of the cilium-associated Shh receptor complex. Mice heterozygous for patched homolog 1 mutations, like heterozygous patched 1 humans, have a higher incidence of Shh subgroup medulloblastoma (MB) and other tumors. Cerebellar cells bearing primary cilia were identified during postnatal development and in adulthood in two mouse strains with altered Shh signaling: a G-protein-coupled receptor 37-like 1 null mutant and an MB-susceptible, heterozygous patched homolog 1 mutant. In addition to granule and Purkinje neurons, primary cilia were also expressed by Bergmann glia astrocytes in both wild-type and mutant animals, from birth to adulthood. Variations in ciliary number and length were related to the different levels of neuronal and glial cell proliferation and maturation, during postnatal cerebellar development. Primary cilia were also detected in pre-neoplastic MB lesions in heterozygous patched homolog 1 mutant mice and they could represent specific markers for the development and analysis of novel cerebellar oncogenic models.

Keywords Gpr37l1 · Bergmann glia · Primary cilium · Medulloblastoma

Introduction

Primary cilia are microtubule-structured organelles that extend from the cell's surface and are crucially involved in sensing and transducing molecular and mechanical extracellular stimuli (Singla and Reiter 2006). Intracellular signaling provoked by ciliary activity and its alteration is distinctly tissue and cell type dependent. In particular, primary cilia are critically required for mammalian brain development, controlling the activation and modulation of specific neuronal mitogenic and developmental signals, such as those of the sonic hedgehog (Shh)- and wingless type-dependent pathways (Han et al. 2008; Gerdes et al. 2007).

The development and differentiation of the cerebellum involve a complex set of regulatory pathways that are only partially understood (Sotelo 2004). In the earliest postnatal stage, cerebellar Purkinje neurons secrete sonic hedgehog protein (Shh), which stimulates the proliferation of neuronal granule cell precursors (GCPs) in the external granule layer (EGL) (Dahmane and Ruiz i Altaba 1999; Wechsler-Reya and Scott 1999; Wallace 1999). Shh also promotes the postnatal maturation/differentiation of Bergmann glia

Chiara Di Pietro, Daniela Marazziti, and Gina La Sala have contributed equally to this work.

Electronic supplementary material The online version of this article (doi:10.1007/s10571-016-0354-3) contains supplementary material, which is available to authorized users.

✉ Daniela Marazziti
daniela.marazziti@cnr.it

[1] Institute of Cell Biology and Neurobiology, Italian National Research Council (CNR), EMMA-INFRAFRONTIER-IMPC, 00015 Monterotondo Scalo, Rome, Italy

astrocytes (Dahmane and Ruiz i Altaba 1999). During postnatal development, both glial astrocytes and GCPs express high levels of Shh pathway components, such as the primary cilium-associated, transmembrane transporter-like patched homolog 1 (Ptch1) and the 7-membrane span smoothened (Smo) proteins (Vaillant and Monard 2009; Ruat et al. 2012). Shh proliferative signals are regulated by several factors, including Ptch1, its primary co-receptor component (Allen et al. 2011; Izzi et al. 2011). The binding of Shh to the Ptch1 complex leads to ciliary translocation and derepression of Smo, thus triggering the intracellular transcriptional activation of several proliferation-related genes (Ho and Scott 2002).

The vertebrate G-protein-coupled receptor 37 and 37-like 1 (*Gpr37* and *Gpr37l1*) genes are highly expressed in brain tissues and encode 7-transmembrane span proteins with amino acid sequence homology to G-protein-coupled receptors of the endothelin and gastrin releasing/bombesin peptides (Marazziti et al. 1997, 1998; Valdenaire et al. 1998). The secreted cytoprotective glycoprotein prosaposin and derived peptides were found to interact in vitro with both putative receptors (Meyer et al. 2013). The mammalian Gpr37l1 protein is specifically expressed in newborn and adult cerebellar Bergmann glia astrocytes. Genetic ablation of Gpr37l1 results in altered expression of Shh pathway markers, reduced GCP proliferation, and precocious maturation of Bergmann astrocytes and Purkinje neurons (Marazziti et al. 2013). The Gpr37l1 protein has also been identified as a modulator of neuronal primary ciliogenesis (Kim et al. 2010) and it interacts and colocalizes with Ptch1 in mouse Bergmann glia cilia (Marazziti et al. 2013), suggesting that it may be directly involved in regulating Shh–Ptch1–Smo ciliary signaling.

Cerebellar medulloblastomas (MBs) have the highest incidence among malignant brain tumors of childhood, with maximal occurrence between 4 and 7 years of age. Certain types of MB are caused by mutations that provoke the constitutive activation of the cerebellar Shh–Ptch1 pathway, resulting in GCP over-proliferation and malignant transformation (Gerber et al. 2014). Loss-of-function mutations of the human patched 1 (*PTCH1*) orthologue gene are a major risk factor for the Shh subgroup of cerebellar MBs. Mice heterozygous for loss-of-function *Ptch1* mutations, like heterozygous *PTCH1* humans, have a higher incidence of MBs, as well as other tumors. Murine homozygous *Ptch1* mutants die between embryonic day (E) 9.0 and E10.5, with widespread nervous system defects (Goodrich et al. 1997). Heterozygous $Ptch1^{+/-}$ animals can survive to adulthood, although, on average, 20 % develop MBs (Goodrich et al. 1997), with continued Shh pathway activation, proliferation of GCP, and expression of several markers very similar to the ones found in human MBs (Corcoran and Scott 2001; Wetmore et al. 2000). Preneoplastic MB lesions have been described in $Ptch1^{+/-}$ mice (Goodrich et al. 1997; Kim et al. 2003; Oliver et al. 2005). They are specifically recognized as foci expressing the monoclonal antibody Ki67 antigen (Ki67) and actively investigated as possible targets for precocious detection of oncogenic transformation (Matsuo et al. 2013).

This study examined the localization and distribution of primary cilia during cerebellar development and adulthood in wild-type mice and $Gpr37l1^{-/-}$ homozygous null animals, with precocious down-regulation of Shh signaling and GCP proliferation (Marazziti et al. 2013). The results of this analysis were compared with the experimental data obtained with a $Ptch1^{+/-}$ MB-susceptible heterozygous line (Marazziti et al. 2013; Hahn et al. 1998), which shows opposite phenotypic characteristics, with increased Shh pathway activation and GCP proliferation, from early postnatal through adult ages.

The experimental results showed that, in addition to GCP and Purkinje cells, primary cilia in wild-type and mutant strains were also found expressed by Bergmann glia (from postnatal day P0 to adulthood). Comparison of $Gpr37l1^{-/-}$ and wild-type cerebellar samples revealed that primary cilia's amount and distribution correlate with the different extent of neuronal and glial cell proliferation and maturation. In $Ptch1^{+/-}$ mice, primary cilia were also found from P16 in pre-neoplastic MB lesions, indicating that they may represent specific markers for the study of oncogenic initiation and progression and the development and analysis of novel cerebellar oncogenic models.

Materials and Methods

Animals and Housing

Hetero- and homozygous *Gpr37l1* knock-out mutant mice ($Gpr37l1^{+/-}$ and $Gpr37l1^{-/-}$; MGI allele symbol: Gpr37l1<tm1.2Gtva>; MGI accession no.: 5439169) and their wild-type littermates with a mixed genetic background (75 % C57BL/6J; 25 % 129S/SvEv) were generated and used as previously described (Marazziti et al. 2013). Heterozygous *Ptch1* knock-out mutant mice ($Ptch1^{+/-}$; MGI allele symbol: Ptch1<tm1Zim>; MGI accession ID: 1857935; (Hahn et al. 1998), with a mixed genetic background (129S2/SvPas original background, backcrossed >5 times to C57BL/6), were provided by the European Mouse Mutant Archive (EMMA) Core Structure (Monterotondo, Italy; strain accession no.: EM:00159; https://www.infrafrontier.eu/search?keyword=00159).

After weaning, mice were housed by litter of the same sex, 3–5 per cage, and maintained in a temperature-controlled room at 21 ± 2 °C, on a 12-h light–dark cycle (lights on at 07:00 a.m.), with food and water available ad libitum. All

animals were born and bred in a specific pathogen-free facility and were subjected to experimental protocols, as reviewed and approved by the Ethical and Scientific Commission of Veterinary Dept. of the Italian Ministry of Health, according to the ethical and safety rules and guidelines for the use of animals in biomedical research provided by the Italian laws and regulations, in application of the relevant European Union's directives (no. 86/609/EEC and 2010/63/EU).

Antigens and Antibodies for Immunofluorescence Labeling

The materials used in this study were as follows: ADP-ribosylation factor-like 13B (Arl13b): UCDavis/NIH NeuroMab Facility monoclonal antibody, clone N295B/66 (mArl13b), 1:500 and Proteintech polyclonal antiserum (pArl13b), 1:1000; brain lipid-binding protein (Blbp): Millipore polyclonal antiserum, 1:100; 5-bromo-2′-deoxyuridine (BrdU): Millipore monoclonal antibody, clone BU-1, 1:100; calbindin 1 (Calb1/CalbD-28K): Sigma-Aldrich monoclonal antibody, clone CB-955, 1:200; contactin 2 (Cntn2/TAG-1): R&D Systems polyclonal antiserum, 1:100; intraflagellar transport 88 (Ift88): Proteintech polyclonal antiserum, 1:50; Gpr37l1: Mab Technologies monoclonal antibody, clone 7-4A1 sc-B12, 1:100; proliferating cell nuclear antigen (Pcna): Thermo Pierce monoclonal antibody, clone PC10, 1:150; Ptch1: Santa Cruz Biotechnology polyclonal antiserum; 1:50; Ki67 antigen (Ki67): ThermoFisher polyclonal antiserum, 1:100; and SRY (sex-determining region Y)-box 9 (Sox9): Millipore polyclonal antiserum, 1:100; γ-tubulin (Sigma-Aldrich monoclonal antibody, clone GTU-88, 1:400).

Immunofluorescence and Quantitative Analysis

De-paraffined mid-vermal sections of age-matched brains from C57BL/6J wild-type or mutant male mice and their wild-type littermates were processed for immunofluorescence labeling and 4′, 6-diamidino-2-phenylindole (DAPI) nuclear staining, according to standard protocols. Fluorescence micrographs were acquired with a TCS SP5 laser scanning confocal microscope (Leica Microsystems) using manufacturer's imaging software. Quantitative image analysis was performed with the Imaris 5.0.2 software (Bitplane). For each section, the total number of cilia (identified as shown in Fig. 2a) in the entire sectioned area of the EGL or Purkinje cell layer (PCL) was counted and normalized by the layer length. The average values of cilium length and normalized total number were calculated upon analysis of at least three non-adjacent sections from three (representative) cerebellar lobes of three animals per genotype and age group. Total cilium counts were about 25,000 in EGL and 8000 in PCL and they did not significantly differ between the two genotypes. Cilium length measurements were performed on about 270 and 360 cilia per genotype and age group. The average ratio of Bergman glial cells versus Purkinje neurons was found to be about 8–10 to 1 in all analyzed samples, independent of the genotype or age group. Sections of similar size in similar regions were chosen, analyzed, and compared. All measurements were conducted with the observer blind to the identity of the slides. Images from a representative experiment are shown.

In Vivo Proliferation Assays and Data Analysis

P3, P5, or P7 *Gpr37l1*$^{-/-}$ and wild-type male littermates received a single BrdU injection (0.1 mg/g body weight) 2 h prior to euthanasia. Brains were dissected and tissue preparation and processing was performed as described above. Double immunofluorescence labeling was performed using anti-BrdU and anti-Blbp antibodies. Fluorescence micrographs were acquired with a motorized LMD7000 microscope (Leica Microsystems) using the manufacturer's imaging software. Quantitative analysis of doubly positive cells was performed with the ImageJ software. Experiments were performed in at least three animals per genotype and age group. Sections of similar size in similar regions were chosen and analyzed. The percentage of Blbp- and BrdU-double-positive over BrdU-positive cells in the PCL was calculated upon cell counting in the entire sectioned area of at least three non-adjacent sections from each mouse. All measurements were performed with the observer blind to the identity of the slides.

Pre-neoplastic Lesion Analysis

Cerebella from P16 and P25 *Ptch1*$^{+/-}$ pups were harvested as described above. The entire cerebellum from each animal was serially sectioned. To identify pre-neoplastic lesions for each cerebellum, every fifth slide (12–14 slides per cerebellum) was stained with Ki67, Arl13b, and DAPI. Images of the lesions were taken on TCS SP5 laser scanning confocal microscope (Leica Microsystems) using manufacturer's imaging software.

Western Blot Analysis

Protein extracts were prepared from the cerebella of *Gpr37l1*$^{-/-}$ or wild-type male pups at different postnatal developmental stages (P5, P10, and P15) or adulthood. The tissue samples were homogenized in lysis buffer (120 mM NaCl, 20 mM Hepes, 5 mM EDTA, 10 % glycerol, 1 % Triton X-100, Roche complete protease inhibitors), cleared by centrifugation, and the protein content of the

supernatant was quantified by Bio-Rad DC Protein Assay (Bio-Rad). Protein samples (50 μg) were separated by SDS/PAGE and analyzed by Western blot, according to standard protocols. Protein antigens were labeled with primary antibodies specific for Arl13b (Proteintech polyclonal antiserum, 1:1000) and α-tubulin (Sigma monoclonal antibody, clone DM 1A, 1:1000). Horseradish peroxidase-conjugated secondary antibodies, specific for mouse (Amersham) or rabbit (Cell Signaling) immunoglobulins, were used, following the manufacturer's instructions. The blotted membranes were then processed for chemiluminescence detection with an ECL PRIME kit (Amersham), exposed and imaged (ChemiDoc XRS+ Imager; Bio-Rad).

Statistical Analysis

All data were analyzed by *t* test, simple factorial ANOVA with genotype and age as between-subject factors using StatView 5.0 PowerPC software (SAS Institute Inc.). Level of significance was set at $P \leq 0.05$.

Results

Primary Cilia in Cerebellar Bergmann Astrocytes During Postnatal Development and Adulthood

The presence and distribution of primary cilia in the murine cerebellum throughout postnatal development and at adult age were investigated by morphological and immunohistological analysis of sagittal sections from wild-type C57BL/6J mouse at various postnatal stages and adulthood, following previous analysis on cerebellar samples from P5 pups of mixed background (C57BL6/J; 129S/SvEv) (Marazziti et al. 2013). Cilia were specifically stained with a monoclonal antibody or a polyclonal antiserum against the specific ciliary marker Arl13b (Caspary et al. 2007; Larkins et al. 2011) both producing an identical pattern of immunoreactivity (Fig. 1c). Arl13b marked ciliary membranes (Fig. 1a–c), while specific γ-tubulin immunolabeling was localized to the microtubular basal bodies from where primary cilia emerge (Fig. 1c). Primary cilia were extensively detected in the EGL (in proliferating Pcna-positive and in post-mitotic TAG-1-positive neurons) from P5 to P15 and in the PCL from P5 to adulthood (Fig. 1a, b), while only scattered ciliary staining was found in internal granule layer (IGL), at any sampled age. These findings were in agreement with previous reports on the cerebellar distribution of other ciliary markers, at distinct pre- and postnatal stages (Chizhikov et al. 2007; Spassky et al. 2008). The Arl13b staining was also confirmed by double immunolabeling of Ift88, a specific marker of primary cilia axonemes during mammalian development and disease (Pazour et al. 2000); Fig. S1a–c). The pattern of expression of the ciliary markers was similar from anterior to posterior regions of the cerebellum. Double immunolabeling of adult PCL samples with antibodies against Arl13b and cell type-specific markers for Purkinje neurons (Calb) or Bergmann glia astrocytes (Sox9 or Blbp) indicated that in adulthood primary cilia extend with comparable density from both cell types (Fig. 1c). The same results were obtained with double immunolabeling of postnatal cerebellar samples from P0 to P20 (Fig. 2a and data not shown). Thus, the application of specific immunomarkers unequivocally shows that Bergmann glia astrocytes also possess primary cilium throughout postnatal development and in adulthood, alongside neuronal GCPs and Purkinje cells (Spassky et al. 2008; Bishop et al. 2007).

Primary Cilium Number and Length During Postnatal Cerebellum Development

Cerebellar GCP proliferation requires functional primary cilia and sustained Shh-mediated mitogenic signaling (Han and Alvarez-Buylla 2010). Genetic ablation of the Ptch1-associated Gpr37l1 receptor results in the premature down-regulation of GCP proliferation and post-mitotic differentiation and precocious maturation of Bergmann glial fibers and differentiation of Purkinje neurons and concomitant alterations of the Shh–Ptch1–Smo signaling pathway (Marazziti et al. 2013). Following immunolabeling of Arl13b (Fig. 2a), the amount, distribution, and length of primary cilia were studied in cerebellar sections from $Gpr37l1^{+/+}$ and $Gpr37l1^{-/-}$ pups, at distinct postnatal stages (Fig. 2). The analysis of the average number of primary cilia in the GCP-enriched EGL of $Gpr37l1^{+/+}$ and $Gpr37l1^{-/-}$ pups showed significant differences between the two genotype groups (Fig. 2b). At P5, both genotypes showed a similar amount of primary cilia, while P10 null mutants exhibited a significant reduction with respect to wild-type controls (*t* test: $t_{(1,5)} = 4.31$, $P = 0.0076$). Both genotype groups had a comparable decrease at P15 (ANOVA: effect of age, $F_{(2,13)} = 67.07$, $P < 0.0001$). Consistent results were obtained from the analysis of PCL, which is enriched in Bergmann astrocytes and Purkinje neurons and also in migrating granule neurons from P5 to P15. $Gpr37l1^{-/-}$ samples showed a marked increase in cilium number at P5 (*t* test: $t_{(1,4)} = -3.10$, $P < 0.05$) and a significant decrease at P10 (*t* test: $t_{(1,4)} = 4.36$, $P < 0.05$), compared to wild-type controls (ANOVA: effect of age, $F_{(3,18)} = 22.82$, $P < 0.0001$; effect of genotype, $F_{(1,18)} = 0.79$, $P = 0.38$, not significant (NS); age × genotype, $F_{(3,18)} = 4.71$, $P = 0.013$).

Ciliary axoneme lengthening directly influences cell cycle time and its reduction, as well as increases axoneme

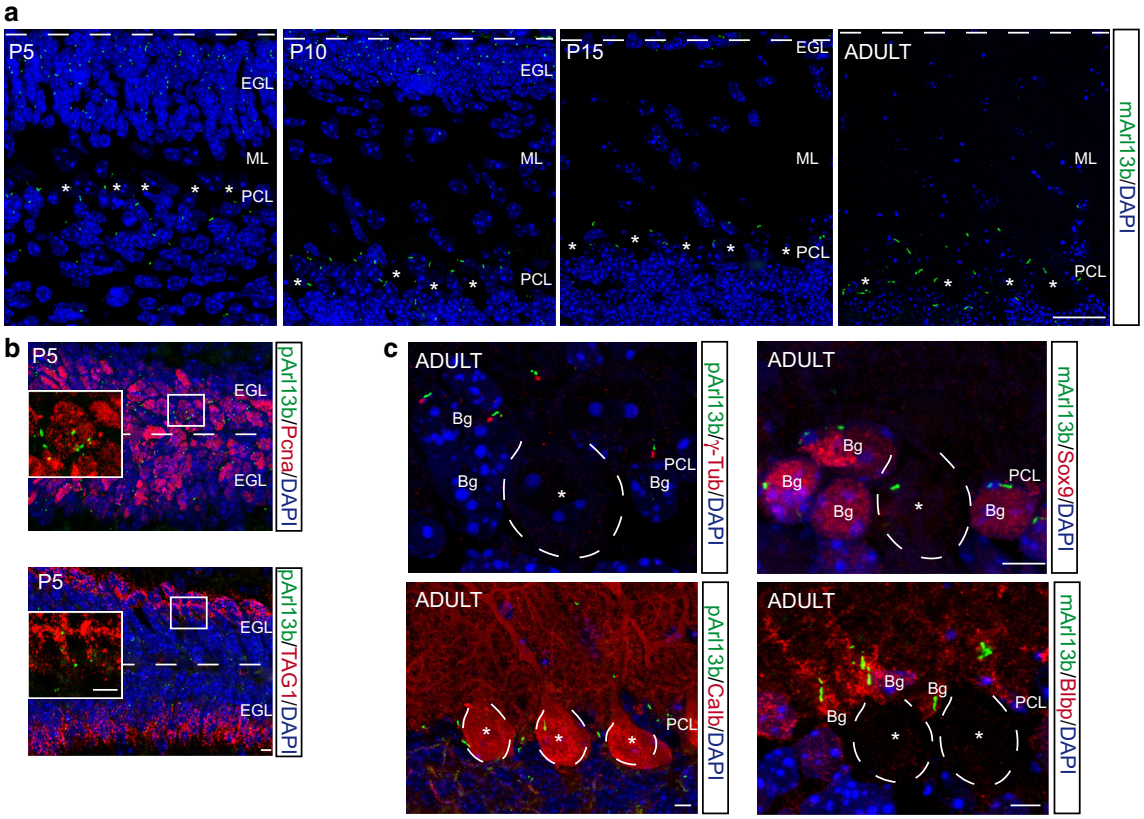

Fig. 1 Staining of cerebellar primary cilia. **a** Cerebellar immunofluorescence labeling of Arl13b (*green*) and DAPI nuclear staining (*blue*) in P5, P10, and P15 pups and adult wild-type C57BL/6J mice. **b** DAPI staining and double immunofluorescence labeling of Arl13b (*green*) and Pcna (*red*, *upper panel*) or TAG-1 (*red*, *lower panel*) in EGL from P5 wild-type C57BL/6J mice. *Insets* display a higher magnification of *boxed areas*. **c** DAPI staining and double immunofluorescence labeling of Arl13b (*green*) and γ-tubulin (*red*) or calbindin 1 (Calb; *red*) or Sox9 (*red*) or Blbp (*red*) in PCL from adult wild-type C57BL/6J mice. *Scale bars* **a** 25 µm, **b**, **c** 5 µm. *Dashed lines* indicate EGL border (**a**, **b**); *asterisks* and *dashed lines* (**a**, **c**) indicate Purkinje neuron somata. *EGL* external granule layer, *ML* molecular layer, *PCL* Purkinje cell layer, *Bg* Bergmann glial cell, *mArl13b* Arl13b monoclonal antibody, *pArl13b* Arl13b polyclonal antiserum

disassembly, and allows cells to enter S-phase more rapidly (Basten et al. 2013). Comparative analysis of average primary cilium length in EGL and PCL was performed in *Gpr37l1*$^{+/+}$ and *Gpr37l1*$^{-/-}$ samples, from P5 to adulthood (Fig. 2c). Samples from P10 null mutants showed a significant increase in PCL cells (*t* test: $t_{(1,3)} = -3.02$, $P < 0.05$) and a non-statistically significant trend in EGL cells, with respect to wild-type controls. Western blot analysis was performed to monitor possible effects of Gpr37l1 genetic ablation on Arl13b protein expression, which might directly influence cilium assembly and structure (Larkins et al. 2011) and therefore the quantification of ciliary parameters. The experimental results (Fig. S1d) revealed no significant difference in the Arl13b cerebellar protein levels between wild-type and *Gpr37l1* null mutant samples, at all studied postnatal ages (P5, P10, and P15).

Specific variations in ciliary parameters are related to alterations of cell proliferation in the developing mammalian brain and other organs (Wheway et al. 2013; Aguilar et al. 2012). Cerebellar cell proliferation was therefore studied in P3–P7 samples from wild-type or *Gpr37l1*$^{-/-}$ littermates, upon in vivo BrdU incorporation, 2 h post-injection (Fig. 3a). BrdU-positive cells were mainly localized in the EGL and PCL in all samples from both genotypes. A significant reduction in the number of proliferating EGL neurons was detected in *Gpr37l1*$^{-/-}$ P7 samples, as previously reported (Marazziti et al. 2013). Proliferating Bergmann astrocytes in the PCL were identified by BrdU and Blbp double immunofluorescence labeling. Most glial cells were found in a proliferative state in P3 and P5 samples from both genotypes. Null mutant pups exhibited a significantly reduced proportion of BrdU- and Blbp-double-positive cells at P7, in comparison with wild-type littermates (Fig. 3b; ANOVA: effect of age, $F_{(2,12)} = 21.68$, $P = 0.0001$; effect of genotype, $F_{(1,12)} = 15.25$, $P < 0.005$.; age X genotype, $F_{(2,12)} = 8.46$, $P = 0.005$). Thus, the above variations in

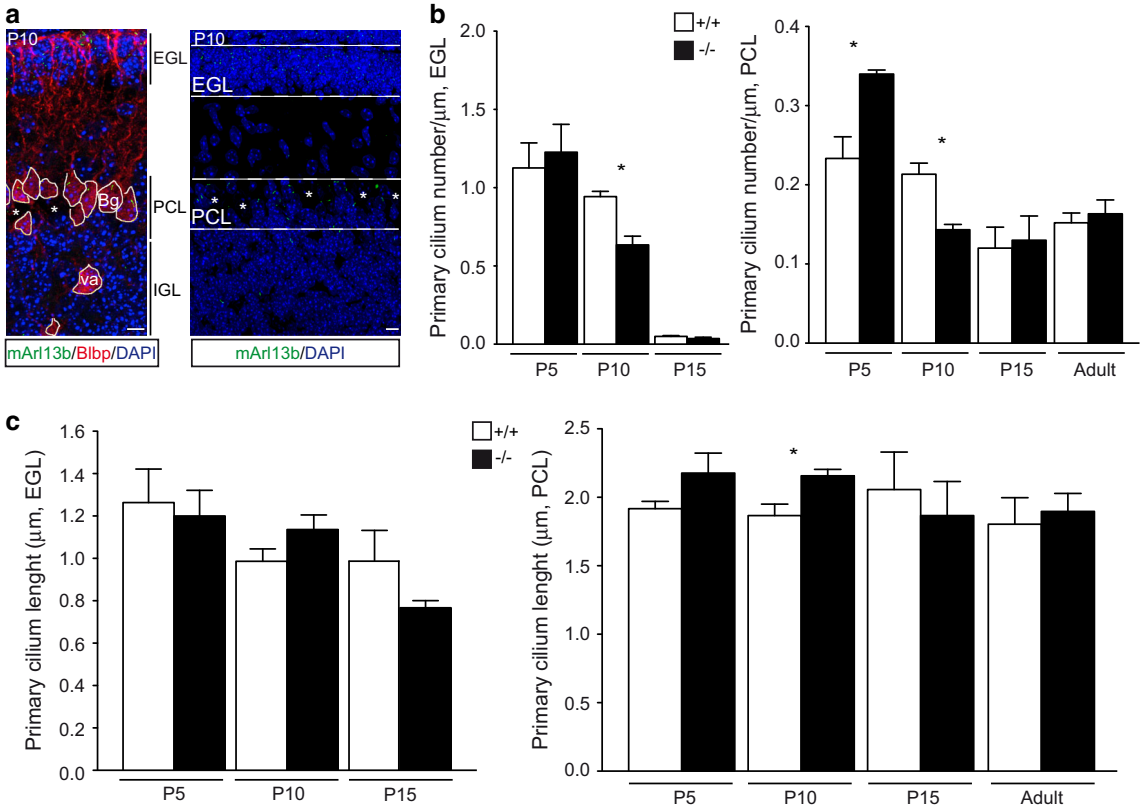

Fig. 2 Quantification of primary cilium length and number in wild-type and *Gpr37l1*$^{-/-}$ mouse cerebella. **a** Representative images of immunofluorescence labeling of Arl13b (*green*) alone (*right*) or in combination with Blbp (*red*; *left*) in cerebellar samples from P10 *Gpr37l1*$^{+/+}$ littermates. *Dashed lines* indicate selected areas corresponding to EGL or PCL, used for primary cilium counting and length measurements; Bergmann glial cell body borders were delimited in *white*; *asterisks* indicate Purkinje neuron somata. *EGL* external granule layer, *PCL* Purkinje cell layer, *Bg Bergmann glial cell body*, *va* velate astrocytes, *mArl13b* Arl13b monoclonal antibody. *Scale bar* 10 µm. **b** Quantification of the average number of primary cilia, normalized by the respective layer length, in EGL and PCL in *Gpr37l1*$^{+/+}$ and *Gpr37l1*$^{-/-}$ littermate mice from P5 to adulthood (mean ± SEM), $n = 3/4$ per group; $^{*}P < 0.05$ +/+ versus −/−, unpaired *t* test. **c** Quantification of the average length of primary cilia in EGL and PCL in *Gpr37l1*$^{+/+}$ and *Gpr37l1*$^{-/-}$ littermate mice from P5 to adulthood (mean ± SEM), $n = 3/4$ per group; $^{*}P < 0.05$ +/+ versus −/−, unpaired *t* test

ciliary parameters are concomitant with the altered proliferation of both cerebellar neurons and glial cells, during the postnatal development of *Gpr37l1*$^{-/-}$ pups.

Primary Cilia in Pre-neoplastic MB Lesions of *Ptch1*$^{+/-}$ Mice

The studied distribution of cerebellar primary cilia in the *Gpr37l1*$^{-/-}$ strain was compared with the results obtained with a *Ptch1*$^{+/-}$ MB-susceptible heterozygous line, which shows opposite phenotypic characteristics, with sustained Shh–Smo pathway activation and GCP hyperproliferation (Hahn et al. 1998). In wild-type pups, the physiologic EGL regression initiates at P14 and is completed by P21, while *Ptch1*$^{+/-}$ mutants retain residual GCPs in the EGL (Thomas et al. 2009). Cerebellar samples from *Ptch1*$^{+/-}$ mice were analyzed at P16 and P25, when pre-tumorigenic MB lesions derived from hyperproliferating GCPs can be distinctly observed and identified in the EGL, as Ki67-positive foci (Matsuo et al. 2013). At both ages, the EGL in normal tissue areas contained residual, Arl13b-positive GCPs (Fig. S2), with very rare or no Ki67-positive neurons at P16 or P25, respectively (Fig. S2b, e). Normal tissue areas also exhibited no alteration of primary cilium distribution in the PCL (Fig. S2c, f). Focal and diffuse hyperproliferating GCPs were present at both ages (Fig. 4a, d) and Ki67-positive foci were readily identified (Fig. 4b, e). Atypical cells in Ki67-positive foci exhibited round or polygonal shape and relatively larger nuclei and double immunofluorescence staining with the Arl13b marker showed that nearly all of them contained a primary cilium (Fig. 4b, c, e, f).

Discussion

Brain glial astrocytes exert crucial functions in regulating neuronal activity by release of chemical transmitters and secretion of protein or peptide factors that modulate

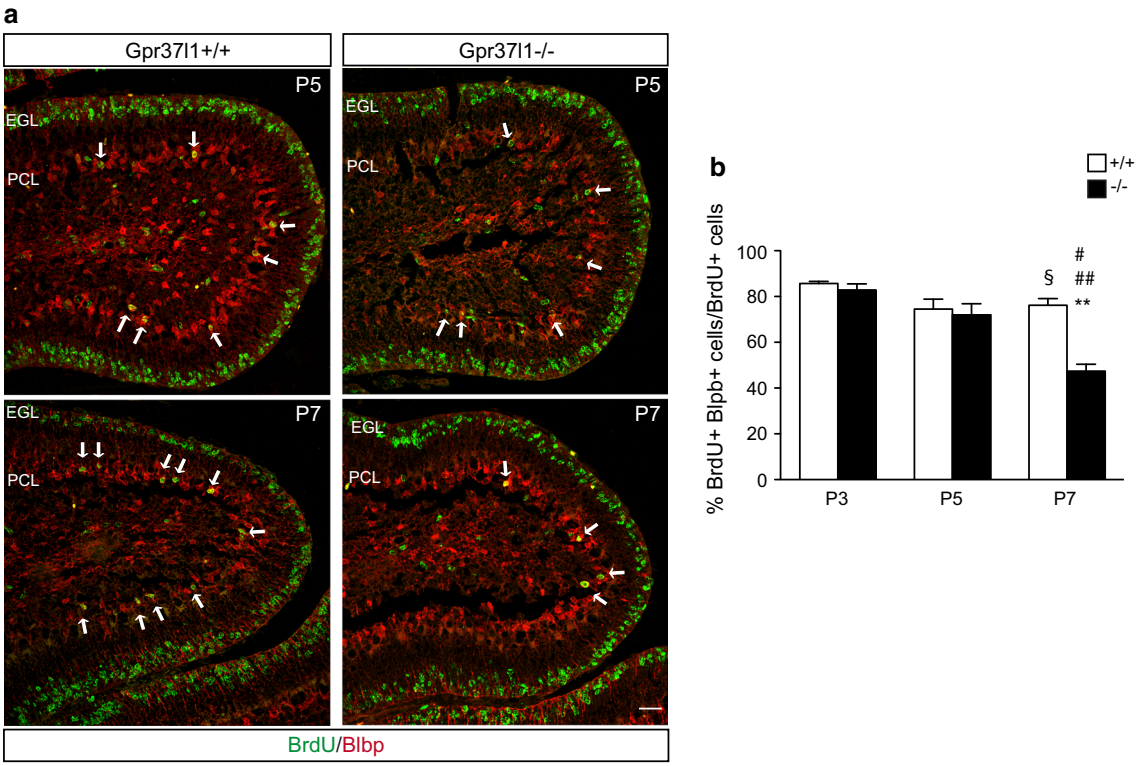

Fig. 3 Postnatal proliferation of cerebellar Bergmann glial cells in wild-type and *Gpr37l1*$^{-/-}$ mice. **a** Representative images of double immunofluorescence labeling of BrdU (*green*) and Blbp (*red*) in cerebellar samples from P5 or P7 *Gpr37l1*$^{+/+}$ and *Gpr37l1*$^{-/-}$ littermates. Double-positive PCL cells are marked by arrowheads. *Scale bar* 10 μm. **b** Percentages of BrdU- and Blbp-double-positive cells over BrdU-positive cells in cerebellar PCL samples from P3, P5, or P7 Gpr37l1$^{+/+}$ and Gpr37l1$^{-/-}$ littermates; (mean ± SEM), $n = 3$ per genotype; $^{**}P < 0.005$ +/+ versus −/−, P7; $^{\#}P < 0.05$, $^{\#\#}P < 0.005$ P7 versus P3 and P5, respectively, in −/− group; $^{\S}P < 0.05$ P3 versus P7 in +/+ group, unpaired *t* test

neuronal gene expression and metabolism (Araque et al. 2001). Astrocyte differentiation and development/maturation is related to specific activation of Shh–Smo signaling cascades (Gallo and Deneen 2014) that occur in many other cell types at primary cilium structures. Primary cilia-like projections have been identified in mouse cerebral cortical astrocytes and cultured hippocampal neurons and astrocytes (Bishop et al. 2007); in addition, mouse subventricular astrocytes have ciliary organelles protruding into the ventricle suggesting that they may sense cerebrospinal fluid factors (Doetsch et al. 1999). In the present study, cerebellar primary cilia were identified by specific immunolabeling of the ciliary membrane marker Arl13b and double immunolabeling of the ciliary axoneme marker Ift88 or the ciliary basal body marker γ-tubulin. By means of combined staining with various cell type-specific immunoreagents, primary cilia were found localized also in non-neuronal, cerebellar Bergmann glial cells, in agreement with the hypothesis that they are required for sensing and transducing extracellular stimuli. Postnatal alterations of ciliary functions, with unregulated activation of Shh–Smo signaling in cerebellar GCPs, can lead to neuronal precursor hyperproliferation and increased occurrence of Shh subgroup MBs, the most common and severely malignant brain tumors of childhood (Han et al. 2009). Primary cilia were therefore studied in detail throughout postnatal cerebellar development and adulthood, in a *Gpr37l1*$^{-/-}$ homozygous null line with reduced GCP proliferation and precocious maturation of Bergmann astrocytes and Purkinje neurons and concomitant alteration of Shh-mediated mitogenic signaling (Marazziti et al. 2013). The comparison of data obtained from *Gpr37l1*$^{-/-}$ and wild-type littermate samples revealed significant variations in cilium's number, distribution, and length in Bergmann glia and neuronal GCPs and Purkinje cells, which were consistent with the cerebellar phenotype reported for the null mutant animals. The significant reduction in the average number of primary cilia in EGL cells of *Gpr37l1*$^{-/-}$ pups at P10 reflects the precocious down-regulation of neuronal GCP proliferation. These findings are in agreement with previous reports showing the involvement of primary cilia in regulating cerebellar development and Shh-induced GCP proliferation (Marazziti et al. 2013; Spassky et al. 2008). A similar decrease was also found in *Gpr37l1*$^{-/-}$ PCL cells at P10, following a marked increase at P5, with a parallel increase in the average cilium length. Bergmann astrocytes

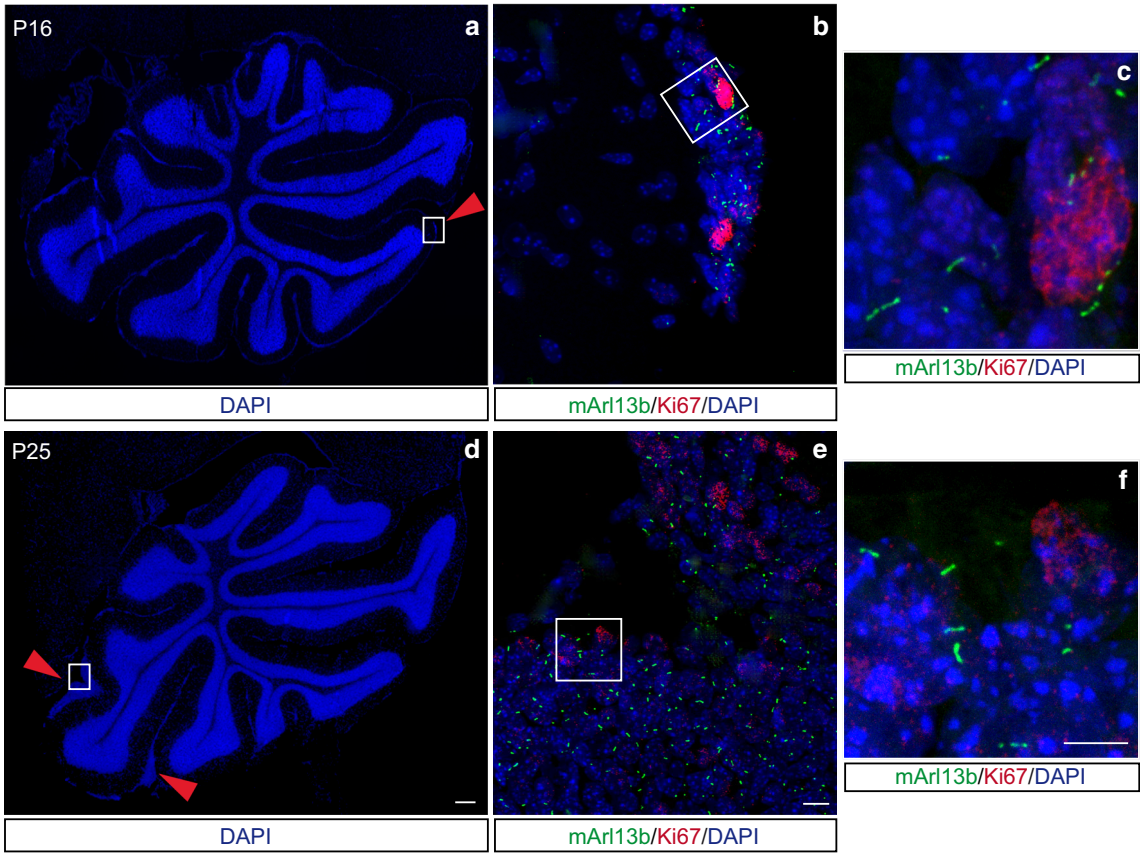

Fig. 4 Staining of cerebellar pre-neoplastic lesions in *Ptch1*$^{+/-}$ mice. DAPI staining (*blue*; **a**–**f**) and Arl13b and Ki67 immunolabeling (*green* and *red*; **b**, **c**, **e**, **f**) of sagittal cerebellar sections from *Ptch1*$^{+/-}$ mice, at P16 (**a**, **b**, **c**) or P25 (**d**, **e**, **f**). **a**, **d** *Red arrows* indicate areas of pre-neoplastic lesions. **b**, **e** Higher magnification of boxed areas in panel **a** and **d**. **c**, **f** Higher magnification of *boxed areas* in panel **b** and **e**. mArl13b, monoclonal antibody anti-Arl13b. *Scale bars* 200 μm (**a**, **d**), 10 μm (**b**, **c**, **e**, **f**)

constitute the vast majority of PCL cells and proliferate during postnatal cerebellar development, while post-mitotic Purkinje neurons do not (Yamada and Watanabe 2002). This study analyzed Bergmann glial postnatal proliferation in null mutant and wild-type animals, by BrdU incorporation experiments. The resulting data confirm and extend previous findings on the precocious differentiation and maturation of cerebellar astrocytes in the absence of the Gpr37l1 protein (Marazziti et al. 2013) and specifically relate the measured variations in ciliary parameters to the concomitant changes of Bergmann glial mitotic activity in the PCL of *Gpr37l1*$^{-/-}$ pups.

The reported data corroborate the hypothesis that prosaposin or other related glycoprotein or peptide ligands could specifically activate postnatal Gpr37l1 signaling in Bergmann glial cells, thus modulating Gpr37l1–Ptch1 interaction and consequently Ptch1-controlled astrocytic ciliary assembly and Shh–Smo mitogenic signaling during the initial stages of cerebellar development (Dahmane and Ruiz i Altaba 1999; Meyer et al. 2013; Sun et al. 1994). Functional cilia can be involved in either promotion or repression of basal cell carcinoma, MB, and other tumor types driven by activating mutations in the Shh–Smo pathway, which lead to hyperproliferative signaling and oncogenic transformation (Han et al. 2009; Basten et al. 2013). Primary cilia were then analyzed in a *Ptch1*$^{+/-}$ heterozygous line, which shows opposite phenotypic characteristics, in comparison to the *Gpr37l1* null mutant strain, as it models constitutive Shh–Smo activation, GCP hyperproliferation, and MB susceptibility, similar to *PTCH1* heterozygous humans (Hahn et al. 1998). Primary cilia were reliably detected in all cells of pre-neoplastic MB foci in *Ptch1*$^{+/-}$ mice. Thus, the specific detection of primary cilia could be usefully applied for the study of early, pre-neoplastic MB lesions and the comparative analysis of novel cerebellar oncogenic models. Precocious identification of ciliated, hyperproliferating cells could in fact be instrumental for the development of more efficient in vivo and ex vivo experimental procedures, aimed at specifically targeting mitogenic ciliary functions and Shh–Smo signaling (Han et al. 2009).

Acknowledgments The authors greatly thank C. Gross for manuscript reading, G. Bolasco of the EMBL-Monterotondo Microscopy Facility for assistance with microscopy, G. D'Erasmo and A. Ventrera for excellent technical assistance, and A. Ferrara and T. Cuccurullo for secretarial work. This study was supported by Consiglio Nazionale delle Ricerche Progetto d'Interesse Strategico Invecchiamento 2012–2016 and European Union Framework Programme (EUCOMM, EUCOMMTools Grants).

Compliance with Ethical Standards

Conflict of interest The authors declare that they have no conflict of interest.

References

Aguilar A, Meunier A, Strehl L, Martinovic J, Bonniere M, Attie-Bitach T, Encha-Razavi F, Spassky N (2012) Analysis of human samples reveals impaired SHH-dependent cerebellar development in Joubert syndrome/Meckel syndrome. Proc Natl Acad Sci USA 109(42):16951–16956. doi:10.1073/pnas.1201408109

Allen BL, Song JY, Izzi L, Althaus IW, Kang JS, Charron F, Krauss RS, McMahon AP (2011) Overlapping roles and collective requirement for the coreceptors GAS1, CDO, and BOC in SHH pathway function. Dev Cell 20(6):775–787

Araque A, Carmignoto G, Haydon PG (2001) Dynamic signaling between astrocytes and neurons. Annu Rev Physiol 63:795–813. doi:10.1146/annurev.physiol.63.1.795

Basten SG, Willekers S, Vermaat JS, Slaats GG, Voest EE, van Diest PJ, Giles RH (2013) Reduced cilia frequencies in human renal cell carcinomas versus neighboring parenchymal tissue. Cilia 2(1):2. doi:10.1186/2046-2530-2-2

Bishop GA, Berbari NF, Lewis J, Mykytyn K (2007) Type III adenylyl cyclase localizes to primary cilia throughout the adult mouse brain. J Comp Neurol 505(5):562–571. doi:10.1002/cne.21510

Caspary T, Larkins CE, Anderson KV (2007) The graded response to Sonic Hedgehog depends on cilia architecture. Dev Cell 12(5):767–778

Chizhikov VV, Davenport J, Zhang Q, Shih EK, Cabello OA, Fuchs JL, Yoder BK, Millen KJ (2007) Cilia proteins control cerebellar morphogenesis by promoting expansion of the granule progenitor pool. J Neurosci 27(36):9780–9789

Corcoran RB, Scott MP (2001) A mouse model for medulloblastoma and basal cell nevus syndrome. J Neurooncol 53(3):307–318

Dahmane N, Ruiz i Altaba A (1999) Sonic hedgehog regulates the growth and patterning of the cerebellum. Development 126(14):3089–3100

Doetsch F, Garcia-Verdugo JM, Alvarez-Buylla A (1999) Regeneration of a germinal layer in the adult mammalian brain. Proc Natl Acad Sci USA 96(20):11619–11624

Gallo V, Deneen B (2014) Glial development: the crossroads of regeneration and repair in the CNS. Neuron 83(2):283–308

Gerber NU, Mynarek M, von Hoff K, Friedrich C, Resch A, Rutkowski S (2014) Recent developments and current concepts in medulloblastoma. Cancer Treat Rev 40(3):356–365

Gerdes JM, Liu Y, Zaghloul NA, Leitch CC, Lawson SS, Kato M, Beachy PA, Beales PL, DeMartino GN, Fisher S, Badano JL, Katsanis N (2007) Disruption of the basal body compromises proteasomal function and perturbs intracellular Wnt response. Nat Genet 39(11):1350–1360. doi:10.1038/ng.2007.12

Goodrich LV, Milenkovic L, Higgins KM, Scott MP (1997) Altered neural cell fates and medulloblastoma in mouse patched mutants. Science 277(5329):1109–1113

Hahn H, Wojnowski L, Zimmer AM, Hall J, Miller G, Zimmer A (1998) Rhabdomyosarcomas and radiation hypersensitivity in a mouse model of Gorlin syndrome. Nat Med 4(5):619–622

Han YG, Alvarez-Buylla A (2010) Role of primary cilia in brain development and cancer. Curr Opin Neurobiol 20(1):58–67

Han YG, Spassky N, Romaguera-Ros M, Garcia-Verdugo JM, Aguilar A, Schneider-Maunoury S, Alvarez-Buylla A (2008) Hedgehog signaling and primary cilia are required for the formation of adult neural stem cells. Nat Neurosci 11(3):277–284. doi:10.1038/nn2059

Han YG, Kim HJ, Dlugosz AA, Ellison DW, Gilbertson RJ, Alvarez-Buylla A (2009) Dual and opposing roles of primary cilia in medulloblastoma development. Nat Med 15(9):1062–1065. doi:10.1038/nm.2020

Ho KS, Scott MP (2002) Sonic hedgehog in the nervous system: functions, modifications and mechanisms. Curr Opin Neurobiol 12(1):57–63. doi:10.1016/S0959-4388(02)00290-8

Izzi L, Levesque M, Morin S, Laniel D, Wilkes BC, Mille F, Krauss RS, McMahon AP, Allen BL, Charron F (2011) Boc and Gas1 each form distinct Shh receptor complexes with Ptch1 and are required for Shh-mediated cell proliferation. Dev Cell 20(6):788–801

Kim JY, Nelson AL, Algon SA, Graves O, Sturla LM, Goumnerova LC, Rowitch DH, Segal RA, Pomeroy SL (2003) Medulloblastoma tumorigenesis diverges from cerebellar granule cell differentiation in patched heterozygous mice. Dev Biol 263(1):50–66

Kim J, Lee JE, Heynen-Genel S, Suyama E, Ono K, Lee K, Ideker T, Aza-Blanc P, Gleeson JG (2010) Functional genomic screen for modulators of ciliogenesis and cilium length. Nature 464(7291):1048–1051. doi:10.1038/nature08895

Larkins CE, Aviles GD, East MP, Kahn RA, Caspary T (2011) Arl13b regulates ciliogenesis and the dynamic localization of Shh signaling proteins. Mol Biol Cell 22(23):4694–4703. doi:10.1091/mbc.E10-12-0994

Marazziti D, Golini E, Gallo A, Lombardi MS, Matteoni R, Tocchini-Valentini GP (1997) Cloning of GPR37, a gene located on chromosome 7 encoding a putative G-protein-coupled peptide receptor, from a human frontal brain EST library. Genomics 45(1):68–77

Marazziti D, Gallo A, Golini E, Matteoni R, Tocchini-Valentini GP (1998) Molecular cloning and chromosomal localization of the mouse Gpr37 gene encoding an orphan G-protein-coupled peptide receptor expressed in brain and testis. Genomics 53(3):315–324

Marazziti D, Di Pietro C, Golini E, Mandillo S, La Sala G, Matteoni R, Tocchini-Valentini GP (2013) Precocious cerebellum development and improved motor functions in mice lacking the astrocyte cilium-, patched 1-associated Gpr37l1 receptor. Proc Natl Acad Sci USA 110(41):16486–16491. doi:10.1073/pnas.1314819110

Matsuo S, Takahashi M, Inoue K, Tamura K, Irie K, Kodama Y, Nishikawa A, Yoshida M (2013) Thickened area of external granular layer and Ki-67 positive focus are early events of medulloblastoma in Ptch1(+)/(−) mice. Exp Toxicol Pathol 65(6):863–873

Meyer RC, Giddens MM, Schaefer SA, Hall RA (2013) GPR37 and GPR37L1 are receptors for the neuroprotective and glioprotective factors prosaptide and prosaposin. Proc Natl Acad Sci USA 110(23):9529–9534. doi:10.1073/pnas.1219004110

Oliver TG, Read TA, Kessler JD, Mehmeti A, Wells JF, Huynh TT, Lin SM, Wechsler-Reya RJ (2005) Loss of patched and disruption of granule cell development in a pre-neoplastic stage of medulloblastoma. Development 132(10):2425–2439. doi:10.1242/dev.01793

Pazour GJ, Dickert BL, Vucica Y, Seeley ES, Rosenbaum JL, Witman GB, Cole DG (2000) Chlamydomonas IFT88 and its

mouse homologue, polycystic kidney disease gene tg737, are required for assembly of cilia and flagella. J Cell Biol 151(3):709–718

Ruat M, Roudaut H, Ferent J, Traiffort E (2012) Hedgehog trafficking, cilia and brain functions. Differentiation 83(2): S97–S104

Singla V, Reiter JF (2006) The primary cilium as the cell's antenna: signaling at a sensory organelle. Science 313(5787):629–633

Sotelo C (2004) Cellular and genetic regulation of the development of the cerebellar system. Prog Neurobiol 72(5):295–339. doi:10.1016/j.pneurobio.2004.03.004

Spassky N, Han YG, Aguilar A, Strehl L, Besse L, Laclef C, Ros MR, Garcia-Verdugo JM, Alvarez-Buylla A (2008) Primary cilia are required for cerebellar development and Shh-dependent expansion of progenitor pool. Dev Biol 317(1):246–259

Sun Y, Witte DP, Grabowski GA (1994) Developmental and tissue-specific expression of prosaposin mRNA in murine tissues. Am J Pathol 145(6):1390–1398

Thomas WD, Chen J, Gao YR, Cheung B, Koach J, Sekyere E, Norris MD, Haber M, Ellis T, Wainwright B, Marshall GM (2009) Patched1 deletion increases N-Myc protein stability as a mechanism of medulloblastoma initiation and progression. Oncogene 28(13):1605–1615. doi:10.1038/onc.2009.3

Vaillant C, Monard D (2009) SHH pathway and cerebellar development. Cerebellum 8(3):291–301. doi:10.1007/s12311-009-0094-8

Valdenaire O, Giller T, Breu V, Ardati A, Schweizer A, Richards JG (1998) A new family of orphan G protein-coupled receptors predominantly expressed in the brain. FEBS Lett 424(3):193–196

Wallace VA (1999) Purkinje-cell-derived Sonic hedgehog regulates granule neuron precursor cell proliferation in the developing mouse cerebellum. Curr Biol 9(8):445–448

Wechsler-Reya RJ, Scott MP (1999) Control of neuronal precursor proliferation in the cerebellum by Sonic Hedgehog. Neuron 22(1):103–114

Wetmore C, Eberhart DE, Curran T (2000) The normal patched allele is expressed in medulloblastomas from mice with heterozygous germ-line mutation of patched. Cancer Res 60(8):2239–2246

Wheway G, Abdelhamed Z, Natarajan S, Toomes C, Inglehearn C, Johnson CA (2013) Aberrant Wnt signalling and cellular over-proliferation in a novel mouse model of Meckel-Gruber syndrome. Dev Biol 377(1):55–66

Yamada K, Watanabe M (2002) Cytodifferentiation of Bergmann glia and its relationship with Purkinje cells. Anat Sci Int 77(2):94–108. doi:10.1046/j.0022-7722.2002.00021.x